FRONTIER ARTICLE

Key Points:
- There is substantial improvement in the comparison between modeled and observed stratospheric temperature trends over the satellite era
- Observations and models show weaker stratospheric cooling since ~1998 when ozone-depleting substances have been declining in the atmosphere
- Larger differences exist between modeled and observed stratospheric temperature trends at high latitudes partly due to internal variability

Revisiting the Mystery of Recent Stratospheric Temperature Trends

Amanda C. Maycock[1], William J. Randel[2], Andrea K. Steiner[3,4], Alexey Yu Karpechko[5], John Christy[6], Roger Saunders[7], David W. J. Thompson[8], Cheng-Zhi Zou[9], Andreas Chrysanthou[1], N. Luke Abraham[10,11], Hideharu Akiyoshi[12], Alex T. Archibald[10,11], Neal Butchart[13], Martyn Chipperfield[1], Martin Dameris[14], Makoto Deushi[15], Sandip Dhomse[1], Glauco Di Genova[16], Patrick Jöckel[14], Douglas E. Kinnison[2], Oliver Kirner[17], Florian Ladstädter[3,4], Martine Michou[18], Olaf Morgenstern[19], Fiona O'Connor[13], Luke Oman[20], Giovanni Pitari[21], David A. Plummer[22], Laura E. Revell[23,24,25], Eugene Rozanov[24,26], Andrea Stenke[24], Daniele Visioni[16,21], Yousuke Yamashita[27,28], and Guang Zeng[19]

[1]School of Earth and Environment, University of Leeds, Leeds, UK, [2]Atmospheric Chemistry, Observations and Modeling Laboratory, National Center for Atmospheric Research, Boulder, CO, USA, [3]Wegener Center for Climate and Global Change, University of Graz, Graz, Austria, [4]Institute for Geophysics, Astrophysics, and Meteorology/Institute of Physics, University of Graz, Graz, Austria, [5]Finish Meteorological Institute, Helsinki, Finland, [6]Earth System Science Center, University of Alabama in Huntsville, Huntsville, AL, USA, [7]Met Office, Exeter, UK, [8]Department of Atmospheric Science, Colorado State University, Fort Collins, CO, USA, [9]National Oceanographic and Atmospheric Administration, Washington, DC, USA, [10]Department of Chemistry, University of Cambridge, Cambridge, UK, [11]National Centre for Atmospheric Science, Cambridge, UK, [12]Center for Global Environmental Research, National Institute for Environmental Studies, Tsukuba, Japan, [13]Met Office Hadley Centre, Exeter, UK, [14]Deutsches Zentrum für Luft- und Raumfahrt, Institut für Physik der Atmosphäre, Oberpfaffenhofen, Germany, [15]Meteorological Research Institute, Tsukuba, Japan, [16]Center of Excellence CETEMPS, Università dell'Aquila, L'Aquila, Italy, [17]Steinbuch Centre for Computing, Karlsruhe Institute of Technology, Karlsruhe, Germany, [18]Météo-France/CNRS, Toulouse, France, [19]National Institute of Water and Atmospheric Research (NIWA), Wellington, New Zealand, [20]NASA Goddard Space Flight Center, Greenbelt, MD, USA, [21]Department of Physical and Chemical Sciences, Università dell'Aquila, L'Aquila, Italy, [22]Climate Research Branch, Environment and Climate Change Canada, Montreal, Quebec, Canada, [23]Bodeker Scientific, Christchurch, New Zealand, [24]Institute for Atmospheric and Climate Science, ETH Zurich, Zurich, Switzerland, [25]School of Physical and Chemical Sciences, University of Canterbury, Christchurch, New Zealand, [26]Physikalisch-Meteorologisches Observatorium Davos/World Radiation Center, Davos, Switzerland, [27]National Institute of Environmental Studies, Tsukuba, Japan, [28]Now at Japan Agency for Marine-Earth Science and Technology, Yokohama, Japan

Abstract Simulated stratospheric temperatures over the period 1979–2016 in models from the Chemistry-Climate Model Initiative are compared with recently updated and extended satellite data sets. The multimodel mean global temperature trends over 1979–2005 are −0.88 ± 0.23, −0.70 ± 0.16, and −0.50 ± 0.12 K/decade for the Stratospheric Sounding Unit (SSU) channels 3 (~40–50 km), 2 (~35–45 km), and 1 (~25–35 km), respectively (with 95% confidence intervals). These are within the uncertainty bounds of the observed temperature trends from two reprocessed SSU data sets. In the lower stratosphere, the multimodel mean trend in global temperature for the Microwave Sounding Unit channel 4 (~13–22 km) is −0.25 ± 0.12 K/decade over 1979–2005, consistent with observed estimates from three versions of this satellite record. The models and an extended satellite data set comprised of SSU with the Advanced Microwave Sounding Unit-A show weaker global stratospheric cooling over 1998–2016 compared to the period of intensive ozone depletion (1979–1997). This is due to the reduction in ozone-induced cooling from the slowdown of ozone trends and the onset of ozone recovery since the late 1990s. In summary, the results show much better consistency between simulated and satellite-observed stratospheric temperature trends than was reported by Thompson et al. (2012, https://doi.org/10.1038/nature11579) for the previous versions of the SSU record and chemistry-climate models. The improved agreement mainly comes from updates to the satellite records; the range of stratospheric temperature trends over 1979–2005 simulated in Chemistry-Climate Model Initiative models is comparable to the previous generation of chemistry-climate models.

Plain Language Summary A previous analysis by Thompson et al. (2012, https://doi.org/10.1038/nature11579) showed substantial differences between satellite-observed and model-simulated

stratospheric cooling trends since the late 1970s. Here we compare recently revised and extended satellite temperature records with new simulations from 14 chemistry-climate models. The results show much better agreement in the magnitude of stratospheric cooling over 1979–2005 between models and observations. This cooling was predominantly driven by increasing greenhouse gases and declining stratospheric ozone levels. An extended satellite temperature record and the chemistry-climate models show weaker global stratospheric cooling over 1998–2016 compared to 1979–1997. This is due to the reduction in ozone-induced cooling from the slowdown of ozone trends and the onset of ozone recovery since the late 1990s. There are larger differences in the latitudinal structure of past stratospheric temperature trends due to the effects of unforced atmospheric variability. In summary, the results show much better consistency between simulated and satellite-observed stratospheric temperature trends than was reported by Thompson et al. (2012, https://doi.org/10.1038/nature11579) for the previous versions of the satellite record and last generation of chemistry-climate models. The improved agreement mainly comes from updates to the satellite records, while the range of simulated trends is comparable to the previous generation of models.

1. Introduction

Atmospheric temperature trends are a key marker of externally forced changes in the climate system (e.g., Hartmann et al., 2013). Stratospheric temperatures are affected by a combination of drivers, including changes in concentrations of radiatively active gases, variations in the strength of the Brewer-Dobson circulation, and natural drivers such as changes in solar irradiance and volcanic eruptions (e.g., Seidel et al., 2016). Better understanding of causes of stratospheric trends and whether they are properly represented in climate models also has implications for understanding recent tropospheric climate change (Garfinkel et al., 2017; Gillett & Thompson, 2003). Satellite and radiosonde observations show that over the past several decades the stratosphere has cooled in the global mean (e.g., Randel et al., 2009), in contrast to the observed warming of the troposphere (e.g., Santer et al., 2013). The observed stratospheric cooling over recent decades has been predominantly driven by increasing concentrations of well-mixed greenhouse gases (GHGs) and decreases in stratospheric ozone resulting from emissions of halogenated ozone-depleting substances (ODSs) into the atmosphere (e.g., Aquila et al., 2016; Austin et al., 2009; Mitchell, 2016; Shine et al., 2003). There is also a potentially significant, but more quantitatively uncertain, contribution to cooling of the lower stratosphere from increasing stratospheric water vapor concentrations (e.g., Forster & Shine, 1999; Maycock et al., 2014). Major tropical volcanic eruptions have caused episodic warming that is particularly pronounced in the lower tropical stratosphere (e.g., Lary et al., 1994), but is also evident throughout the stratosphere in the global mean.

The satellite record of stratospheric temperatures extends from late 1978 to the present. The main long-term stratospheric temperature record for climate studies is the Stratospheric Sounding Unit (SSU) covering 1979–2005 and consisting of measurements in three channels with vertical weighting functions spanning the middle to upper stratosphere. Thompson et al. (2012) reported significant disagreement in long-term stratospheric temperature trends in two versions of the SSU record developed by the UK Met Office and NOAA/STAR (National Oceanographic and Atmospheric Administration Center for Satellite Applications and Research; Wang et al., 2012). At the time the causes of the differences in long-term trends between the two versions of the SSU record were unknown. Thompson et al. (2012) also reported differences between stratospheric temperature trends in the two versions of the SSU record and model simulations from the fifth Coupled Model Intercomparison Project and the Chemistry-Climate Model Validation project. On average, the models showed weaker long-term cooling in the upper stratosphere and lower mesosphere (SSU channel 3, ~40–50 km) of around 0.8–0.9 K/decade compared to the cooling trend in both SSU data sets (~1.2 K/decade). In the middle to upper stratosphere (SSU channel 2, ~35–45 km), the modeled cooling trends (~0.6–0.7 K/decade) lay between the best estimates of the cooling trends from the Met Office and NOAA/STAR data sets (~0.4 and 0.9 K/decade, respectively). In the middle stratosphere (SSU channel 1, ~25–35 km), the simulated temperature trends (~0.5 K/decade) were in better agreement with the Met Office SSU data set, while the NOAA/STAR data set showed cooling around a factor of 2 larger (~1 K/decade). The differences between the independent versions of the SSU record and between models and satellite data sets highlighted by Thompson et al. (2012) presented significant challenges both for characterizing observed stratospheric temperature changes and for attributing the changes to specific external or internal climate drivers

(Arblaster et al., 2014). This led to the conclusion in the World Meteorological Organization (WMO)/United Nations Environment Programme (UNEP) 2014 Scientific Assessment of Ozone Depletion that "observed mid- and upper-stratospheric temperatures decreased from 1979 to 2005, but the magnitude of the cooling is uncertain."

Since the Thompson et al. (2012) study, the SSU temperature data sets have been revised and updated by the Met Office (Nash & Saunders, 2013, 2015) and NOAA/STAR (Zou et al., 2014). Seidel et al. (2016) provided a comparison of the updated SSU records and showed that the differences in long-term temperature trends over 1979–2005 are generally smaller than found by Thompson et al. (2012), but some differences between the data sets remain particularly in SSU channels 2 and 3. This study provides a further update to Thompson et al. (2012) by comparing the revised SSU records with new simulations performed by the International Global Atmospheric Chemistry/Stratosphere-troposphere Processes And their Role in Climate (IGAC/SPARC) Chemistry-Climate Model Initiative (CCMI).

Another development since Thompson et al. (2012) is the creation of a number of merged stratospheric temperature data sets that combine the NOAA/STAR SSU record with more recent AMSU-A (Advanced Microwave Sounding Unit-A; McLandress et al., 2015; Zou & Qian, 2016), Microwave Limb Sounder (MLS), or Sounding of the Atmosphere using Broadband Emission Radiometry (SABER; Randel et al., 2016) measurements to create stratospheric temperature records that extend from 1979 to present day. Comparisons of individual chemistry-climate models with these extended satellite records have shown good agreement in global mean stratospheric temperature trends (e.g., Aquila et al., 2016; Randel et al., 2017). Larger differences between model simulations and satellite data sets have been found in the latitudinal structure of stratospheric temperature trends, in part due to the greater contribution from internal atmospheric variability to local temperature variations particularly at high latitudes (Randel et al., 2017). The extended SSU records have allowed a first comparison of stratospheric temperature trends between the period when atmospheric ODS abundances, and hence ozone depletion, were increasing in time (~pre-1998) and the period when ODS concentrations in the atmosphere have been declining (~post-1998; e.g., WMO, 2014). Randel et al. (2016) and Zou and Qian (2016) showed weaker observed stratospheric cooling trends in all SSU channels over 1998–2015 compared to 1979–1997, which was captured by the CESM1(WACCM) chemistry-climate model (Randel et al., 2017). Solomon et al. (2017) analyzed output from CESM1(WACCM) and showed that stratospheric ozone and temperature trends associated with the Antarctic ozone hole mirror one another in the periods before and after 1998, suggesting that the changes in stratospheric temperature trends since the late 1990s have been at least partly driven by changes in ozone photochemistry associated with declining atmospheric ODSs. In the lower stratosphere (Microwave Sounding Unit channel 4 [MSU4], ~13–22 km), cooling has approximately ceased since the late 1990s (Ferraro et al., 2015; Khaykin et al., 2017). Model analyses suggest that ODS trends were the dominant driver of global lower stratospheric cooling in the MSU4 channel layer from the late 1970s to the mid-1990s (Arblaster et al., 2014) and that changes in the Brewer-Dobson circulation in response to ODSs may have played a role in driving the observed lower stratospheric temperature trends (Polvani et al., 2017). The second focus of this study is therefore to compare model and observed stratospheric temperature trends before and after 1998 to distinguish trends in the period when ozone depletion was increasing and the period when ozone recovery has been detected (e.g., Harris et al., 2015).

2. Methods

2.1. Satellite Temperature Data Sets

The study presents results of layer mean stratospheric temperatures from several satellite data sets processed and published by different research groups.

The NOAA/STAR SSU data set version 3.0 is provided as monthly mean values on a $2.5° \times 2.5°$ longitude $\times$ latitude grid covering the period 1979–2016 (Zou & Qian, 2016). The data set has been extended from 2006 to the near-present using AMSU-A observations by mapping the AMSU-A channel vertical weighting functions onto the SSU channel weighting functions (Zou & Qian, 2016). The SSU channels 1, 2, and 3 weighting functions peak at around 30, 38, and 45 km, respectively. Comparisons are also presented with the reprocessed Met Office SSU data set (Nash & Saunders, 2015), which is provided as 6-month and global averages for the period 1979–2005. The reprocessed NOAA/STAR data set was shown to have a more consistent

Table 1
The CCMI Models and the Number of Ensemble Members Used for Each Experiment in This Study

Model	Ocean	refC2	senC2fODS	senC2fGHG	Reference
CCSRNIES-MIROC3.2	Prescribed	1	1	1	Imai et al. (2013); Akiyoshi et al. (2016)
CESM1-WACCM	Coupled	3	1	1	Marsh et al. (2013); Solomon et al. (2015)
CMAM	Prescribed	1	1	1	Jonsson et al. (2004); Scinocca et al. (2008)
CNRM-CM5–3	Prescribed	1	—	—	Voldoire et al. (2013); Michou et al. (2011); http://www.umr-cnrm.fr/
EMAC (L47/L90)	Pprescribed	1 (L47/L90)	—	1 (L90)	Jöckel et al. (2016)
GEOSCCM	Prescribed	1	—	—	Molod et al. (2012, 2015); Oman et al. (2011, 2013)
HadGEM3-ES	Coupled	1	—	—	Walters et al. (2014); Madec (2008); Hunke and Lipscombe (2008); Morgenstern et al. (2009); O'Connor et al. (2014); Hardiman et al. (2017)
MRI-ESMr1	Coupled	1	—	—	Yukimoto et al. (2011, 2012); Deushi and Shibata (2011)
NIWA-UKCA	Coupled	5	1	1	Morgenstern et al. (2009, 2013); Stone et al. (2016)
SOCOL3	Prescribed	1	—	—	Stenke et al. (2013); Revell et al. (2015)
ULAQ-CCM	Prescribed	3	1	1	Pitari et al. (2014)
UMSLIMCAT	Prescribed	1	1	1	Tian and Chipperfield (2005)
UMUKCA-UCAM	Prescribed	2	—	—	Morgenstern et al. (2009); Bednarz et al. (2016)

*Note.* CCMI = Chemistry-Climate Model Initiative.

representation of vertical coherency in stratospheric temperatures as represented by models than the Met Office SSU data set (Seidel et al., 2016).

Temperatures in the lower stratosphere are measured by the MSU4 (from 1978–2005) and the Advanced Microwave Sounding Unit channel 9 since 1998. This channel has a weighting function that peaks at around 17 km with main contributions from the layer 13–22 km. We present results from the NOAA/STAR MSU4/AMSU-A version 4.0 (Zou et al., 2006), the Remote Sensing Systems v3.3 MSU4/AMSU-A (Mears et al., 2011; Mears & Wentz, 2009), and the UAH (University of Alabama in Huntsville) v6.0 MSU4-AMSU data sets (Christy et al., 2003), which all cover 1979–2016 (see, e.g., Seidel et al., 2016 for a recent detailed comparison of MSU4 data sets).
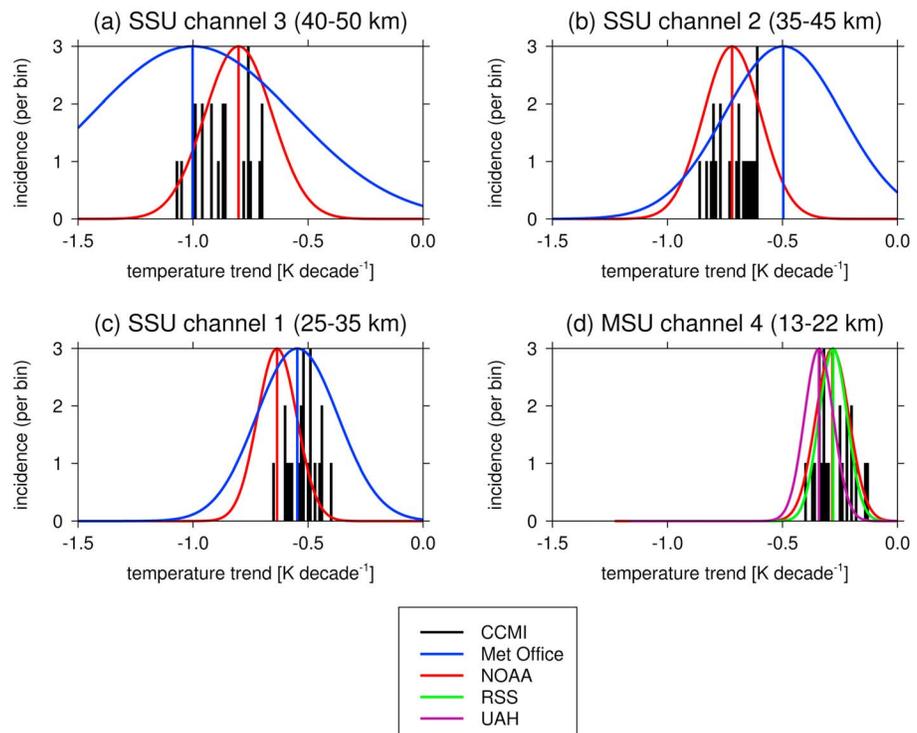
2.2. CCMI Models

The analysis uses zonal and monthly mean temperature output on pressure levels from the CCMI models listed in Table 1 (see Morgenstern et al., 2017, for further details). Data were downloaded from the CCMI Database hosted at the British Atmospheric Data Centre. Data are used from the following experiments (Eyring et al., 2013): refC2, senC2fODS, and senC2fGHG. All experiments span the period 1960–2100 though only the period 1979–2016 is analyzed here.

The models performed a 10-year spin-up from 1950 to 1959 before beginning the simulations from 1960. Concentrations of greenhouse gases (CO_2, N_2O, and CH_4) are prescribed from observations to 2005 and then follow the representative concentration pathway 6.0 scenario (Eyring et al., 2013). Concentrations of ODSs are prescribed according to the WMO (2011) A1 scenario. Some, but not all, models include the effects of spectrally-resolved solar irradiance changes and variations in tropical stratospheric winds associated with the quasi-biennial oscillation (see Morgenstern et al., 2017). Each model performed the refC2 experiment using either an interactive coupled ocean or with prescribed sea surface temperatures (SSTs) and sea ice taken from a separate model simulation (see Table 1). The CCMI refC1 experiment would therefore be a more natural choice to compare with satellite data sets, since the experimental protocol prescribes observed SSTs and sea ice in all models. However, most of the refC1 simulations end in 2009 or 2010 meaning a comparison up to near present day is not possible. Hence, the refC2 experiment is used for our analysis. One main difference between refC1 and refC2, other than the treatment of the ocean state, is the representation of forcing from volcanic aerosols. Most of the CCMI models now include the radiative effects of volcanic aerosols, either by calculating a volcanic aerosol size distribution or assuming a distribution and then deriving radiative heating rates from it. However, there were differences between modeling groups in the interpretation of how volcanic aerosols should be represented in the refC2 experiment (Eyring et al., 2013). Most models did not include heating from volcanic aerosols in the hindcast period, except for CESM1(WACCM), GEOSCCM,
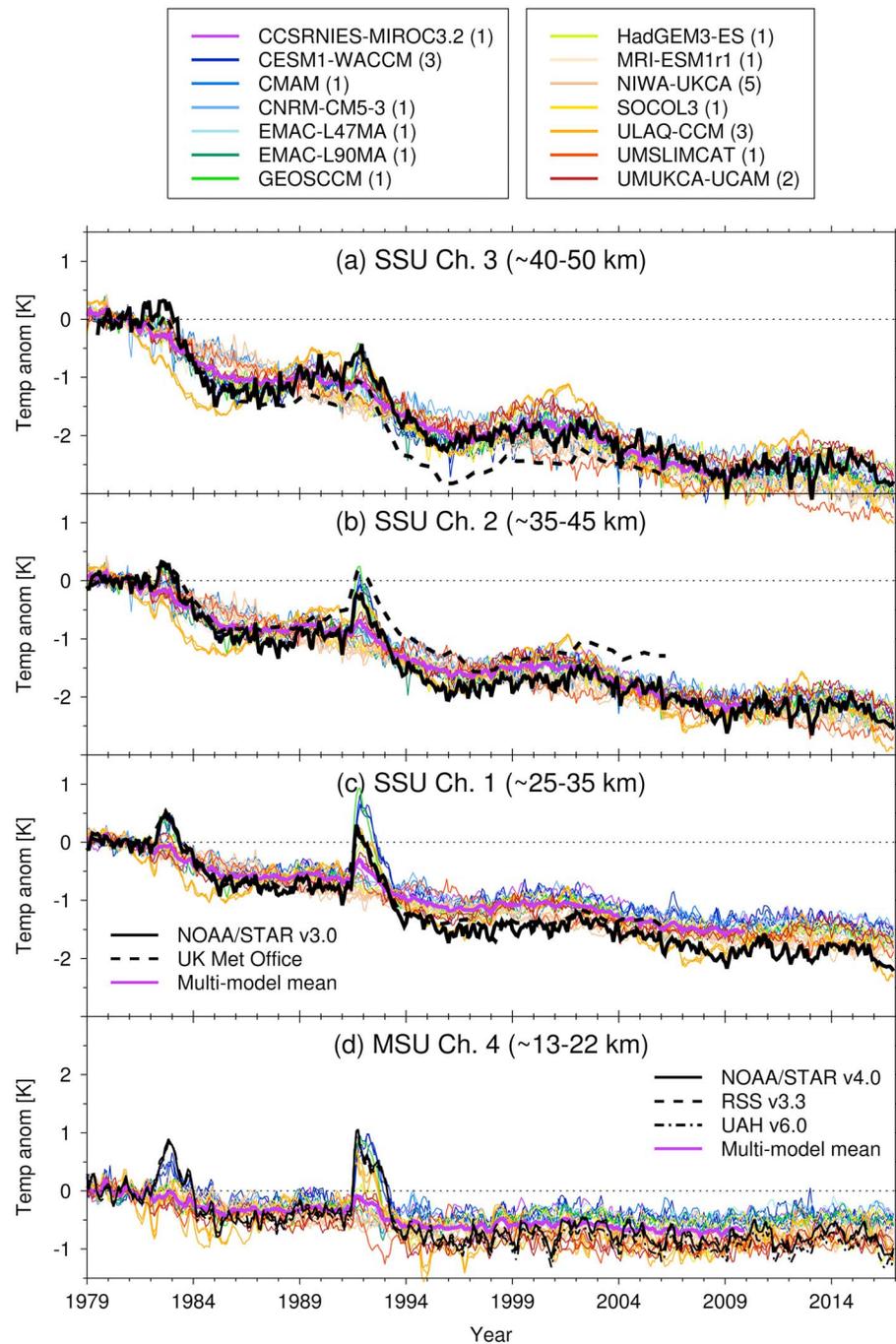
Figure 1. Time series of global monthly mean temperature anomalies (K) for the period 1979–2016 for the data sets and altitude ranges stated in the figure. Anomalies are shown relative to a baseline of 1979–1981. The number of individual ensemble members plotted for each model is shown in the legend. The multimodel mean is shown in thick purple. Note that only the CESM1(WACCM), GEOSCCM, ULAQ-CCM, and UMUKCA-UCAM models include the radiative effects of volcanic aerosols over the hindcast period in the refC2 experiment. Note the UK Met Office SSU data set is shown as 6-month averages. (a) SSU channel 3 (~40–50 km). (b) SSU channel 2 (~35–45 km). (c) SSU channel 1 (~25–35 km). (d) MSU channel 4 (~13–22 km). SSU = Stratospheric Sounding Unit.

ULAQ-CCM, and UMUKCA-UCAM, whereas in the refC1 experiment which only covers the hindcast period, most models do include volcanic aerosols. Hence, in most of the refC2 simulations analyzed here there is no lower stratospheric heating simulated following the large El Chichón and Mount Pinatubo eruptions, and any effects on stratospheric temperatures from secular trends in volcanic aerosols will not be

Figure 2. Trends in global-mean stratospheric temperatures between 1979 and 2005 are shown for (a–c) SSU channels and (d) MSU channel 4, for the satellite data sets and CCMI models. Trends are calculated from monthly mean data except for the Met Office data set where 6-month averages are used. Satellite-observed trends are denoted by the colored vertical lines. For models with more than one ensemble member, the ensemble mean trend is plotted. The normalized probability distribution functions indicate the confidence ranges on the trend estimates, taking into account the effective number of degrees of freedom in the respective time series. Black bars show the histograms of the trends from the CCMI models. The bin size is 0.01 K/decade. The number of model runs is given in Table 1. Data in the 2 years following the two major volcanic eruptions in the period (El Chichón and Mt Pinatubo) are excluded from the trend analysis. SSU = Stratospheric Sounding Unit; MSU = Microwave Sounding Unit; CCMI = Chemistry-Climate Model Initiative.

captured. Nevertheless, the long-term evolution of global mean stratospheric temperatures in refC2 is comparable to refC1 (see Figure S1 in the supporting information), suggesting that the influence of volcanic aerosols on long-term temperature trends is rather small. Since temperature trends in the observations and the four CCMI models mentioned above would be affected by the occurrence of major volcanic eruptions, the 2-year periods immediately following the major eruptions in the epoch (El Chichón in March 1982 and Mount Pinatubo in June 1991) are excluded from the trend analyses; for consistency this is done for the observations and all of the models. However, we note that including the post-volcanic years in the trend calculations does not have a profound effect on the results.

To explore the drivers of recent stratospheric temperature trends, two further sensitivity experiments from CCMI are examined. The senC2fODS experiment is identical to refC2 except that atmospheric (or surface) concentrations of halogenated ODSs are kept fixed at 1960 levels throughout the experiment. Similarly, in senC2fGHG the concentrations of well-mixed GHGs (CO_2, CH_4, and N_2O) are kept fixed at 1960 levels. These experiments therefore enable a separation of the first-order effects of ODSs and GHGs on stratospheric temperature trends. Note that only a subset of the models ran the senC2fODS and senC2fGHG experiments (see Table 1). For the models that prescribe SSTs and sea ice, the boundary conditions used in the senC2fODS experiment are the same as in refC2, but in the senC2fGHG experiment an average of the period 1955–1964 from refC2 is used, repeating each year (see Eyring et al., 2013; Morgenstern et al., 2017). In contrast, the models with coupled oceans will have a different evolution of SSTs and sea ice in senC2fODS and senC2fGHG compared to refC2 owing to the altered radiative forcing history; however, the committed warming up to the point when ODSs or GHGs are fixed will be captured and may affect stratospheric temperatures in subsequent years.
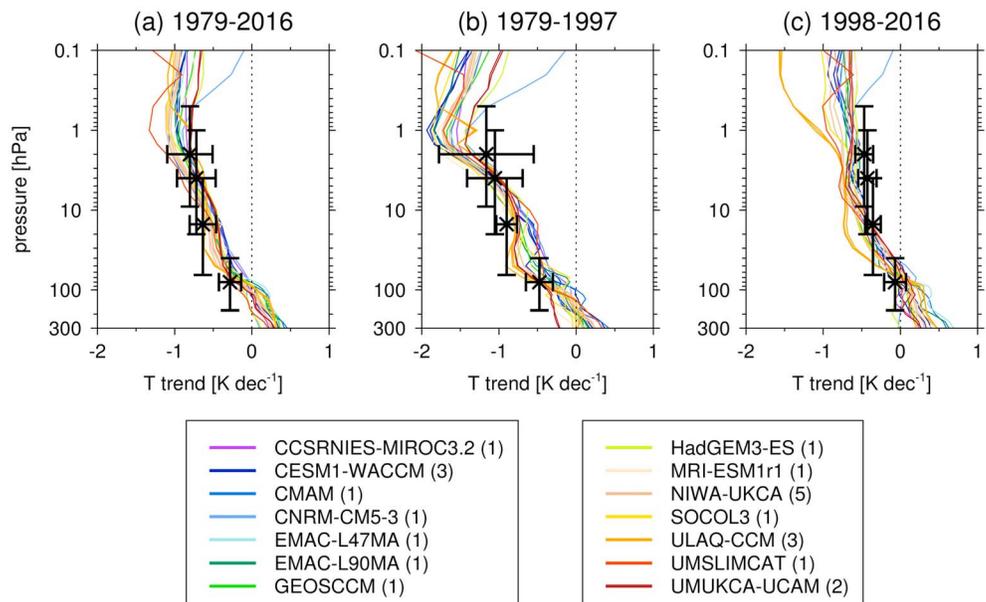
Figure 3. Vertical profiles of global mean annual temperature trends (K/decade) in the SSU-AMSU and MSU4-AMSU NOAA/STAR satellite data set (black bars) and the CCMI models (colors). Trends are calculated for (a) 1979–2016, (b) 1979–1997, and (c) 1998–2016. The number of individual ensemble members plotted for each model is given in the legend. The horizontal whiskers denote 95% confidence intervals on the observed linear trends accounting for the effective number of degrees of freedom in the time series. The vertical whiskers denote the approximate altitude range of the satellite weighting functions. Data in the 2 years following the two major volcanic eruptions in the period (El Chichón and Mt Pinatubo) are excluded from the trend analysis. SSU = Stratospheric Sounding Unit; AMSU = Advanced Microwave Sounding Unit; MSU4 = Microwave Sounding Unit channel 4; NOAA/STAR = National Oceanographic and Atmospheric Administration Center for Satellite Applications and Research; CCMI = Chemistry-Climate Model Initiative.

To produce output from the CCMI models that is comparable to the satellite data sets, the pressure level output is sampled using the vertical global weighting functions for the three SSU channels (ftp://ftp.star.nesdis.noaa.gov/pub/smcd/emb/mscat/data/SSU/SSU_v3.0) and the MSU4/AMSU9 channel covering the upper troposphere/lower stratosphere (C.Z. Zou, personal communication, July 2017). Trends are calculated using least squares linear regression, and confidence intervals on trends are estimated using the standard error of the fit accounting for the effect of lag-1 autocorrelation in the residuals (Santer et al., 2000). To examine the effects of internal variability on stratospheric temperature trends, multiple ensemble members from each model are used where available (see Table 1).

3. Results

3.1. Evolution of Global Stratospheric Temperatures

Figure 1 shows time series of global average temperature anomalies in the three SSU and MSU4 channels. As reported by Seidel et al. (2016), the updated NOAA and Met Office SSU records show greater consistency than the previous versions described by Thompson et al. (2012). Differences do remain, however, with the Met Office data set showing ~0.5 K less cooling in SSU channel 2 between 1979 and 2005, and ~0.5 K more cooling in channel 3, but these differences are smaller than those in Thompson et al. (2012) where they exceeded 1 K in channels 1 and 2. The CCMI multimodel mean generally follows closely the NOAA/STAR data set in SSU channels 2 and 3, with the exception of the periods around the major volcanic eruptions (see section 2.2). In the refC1 experiment (see Figure S1), the CCMI multimodel mean temperature anomalies show better agreement with the satellite data sets in the periods around the major volcanic eruptions, though this reflects averaging across a large spread, with some models not simulating any stratospheric heating from volcanic eruptions and some models strongly overestimating the response. In Figure 1, the CCMI multimodel mean shows larger differences from the Met Office data set in SSU channels 2 and 3. In the low to middle stratosphere (SSU channel 1), the two SSU data sets are in better agreement, but the CCMI multimodel mean shows slightly weaker long-term cooling, on average, compared to the satellite data sets. Of the individual models,

Table 2
Linear Temperature Trends (K/Decade) With 95% Confidence Intervals for Different Data Sets and Periods

Model/dataset	MSU4 (~13–22 km)			SSU1 (~25–35 km)			SSU2 (~35–45 km)			SSU3 (~40–50 km)		
	1979–2005	1979–1997	1998–2016	1979–2005	1979–1997	1998–2016	1979–2005	1979–1997	1998–2016	1979–2005	1979–1997	1998–2016
CCMI	−0.25 ± 0.12	−0.37 ± 0.14	−0.02 ± 0.07	−0.50 ± 0.12	−0.66 ± 0.14	−0.34 ± 0.14	−0.70 ± 0.16	−0.92 ± 0.12	−0.49 ± 0.16	−0.88 ± 0.23	−1.16 ± 0.17	−0.58 ± 0.21
Met Office	—	—	—	−0.55 ± 0.35	−0.82 ± 0.25	—	−0.50 ± 0.50	−0.74 ± 0.77	—	−1.00 ± 0.86	−1.61 ± 0.50	—
NOAA	−0.28 ± 0.14	−0.48 ± 0.17	−0.07 ± 0.14	−0.64 ± 0.17	−0.90 ± 0.14	−0.25 ± 0.10	−0.72 ± 0.25	−1.07 ± 0.26	−0.40 ± 0.11	−0.80 ± 0.29	−1.15 ± 0.53	−0.46 ± 0.11
RSS	−0.28 ± 0.12	−0.45 ± 0.15	−0.08 ± 0.13	—	—	—	—	—	—	—	—	—
UAH	−0.34 ± 0.12	−0.51 ± 0.15	−0.09 ± 0.13	—	—	—	—	—	—	—	—	—

Note. Trends are calculated from monthly mean data except for the Met Office data set where 6-month averages are used. Confidence intervals for the CCMI multimodel mean represent ±2 standard deviations of temperature trends across the different simulations. For the satellite data sets, confidence intervals are based on the uncertainty in the linear regression fit accounting for the effective number of degrees of freedom in each time series (Santer et al., 2000). Note that the confidence intervals are largest for the Met Office data set because 6 times fewer data points are used compared to the other records. The Met Office SSU data set is only available up to 2005, and hence trends are not calculated for 1998–2016. CCMI = Chemistry-Climate Model Initiative; NOAA = National Oceanographic and Atmospheric Administration; UAH = University of Alabama in Huntsville; SSU = Stratospheric Sounding Unit; RSS = Remote Sensing Systems.

ULAQ-CCM shows a much stronger quasi-decadal temperature variability than observed, particularly in the upper stratosphere, which suggests an over estimation of the effect of the 11-year solar cycle on stratospheric temperatures.

Figure 2 shows the trends in global mean monthly temperatures over the period 1979–2005 in the satellite data sets and the CCMI models. This can be compared with Figure 2 of Thompson et al. (2012). Note that the estimated confidence intervals on the trends in the Met Office SSU data set are larger than in the NOAA SSU data set because there are less data points in the regression and because there is a higher autocorrelation in the regression residuals than found for the monthly mean NOAA time series. Given that the updated Met Office data set is available only as 6-monthly averages, this provides poorer statistical constraints on the trends than the previous version analyzed by Thompson et al. (2012), which was provided as monthly mean data.

In the upper stratosphere (SSU channel 3), the CCMI modeled temperature trends range from −0.7 to −1.1 K/decade. There is substantially better agreement between the modeled and observed SSU channel 3 trends than reported by Thompson et al. (2012), who found that both satellite data sets showed stronger upper stratospheric cooling than simulated in most of the models they analyzed. In SSU channel 2, the modeled temperature trends range from −0.6 to −0.8 K/decade, which are also within the uncertainty range of the observed trends. This is again in contrast to the findings of Thompson et al. (2012), who found poor consistency between modeled and observed temperature trends at these altitudes, with the modeled trends lying between the estimated trends from the previous versions of the NOAA and Met Office SSU data sets. In the low to middle stratosphere (SSU channel 1), the modeled trends range from −0.4 to −0.7 K/decade and although these fall within the uncertainty bounds of both SSU data sets, they cluster closer to the best estimate of the trend in the Met Office record and lie below the 50th percentile of the estimated confidence intervals for the NOAA data set. In the lower stratosphere (MSU4), the modeled temperature trends over 1979–2005 range from −0.2 to −0.4 K/decade, which are in good agreement with satellite-observed estimates.

In summary, there are significant improvements in the consistency between modeled and observed trends in SSU layer temperatures compared to the findings of Thompson et al. (2012). These improvements are predominantly from the recent revisions to the SSU records, while the distributions of the modeled trends are similar to the results from the fifth Coupled Model Intercomparison Project and Chemistry-Climate Model Validation project models presented in Thompson et al. (2012). The subsequent analyses in this study focus on the extended NOAA/STAR SSU data set since the Met Office data set is provided as global averages and ends in 2005, when the SSU stopped making measurements, meaning an assessment of temperature trends over the recent past and of the spatial pattern of trends is not possible. For the MSU4 channel, we also show for simplicity only the NOAA/STAR data set, which has similar long-term trends to the RSS data set but somewhat weaker trends than the UAH record.

Figure 3 shows vertical profiles of global mean stratospheric temperature trends over the periods 1979–2016 (Figure 3a), 1979–1997 (Figure 3b), and 1998–2016 (Figure 3c) in the CCMI simulations and satellite data sets. The trends over these periods in the SSU and MSU4 channels for all the data sets along with their 95% confidence intervals are given in Table 2. Over 1979–2016 there is an increase in the magnitude of the cooling trend with height. This is understood to be due to two factors: (1) the effect on stratospheric temperatures from an increase in CO_2 increases with height (e.g., Manabe & Wetherald, 1975) and (2) the vertical profile of ozone depletion which causes a relative maximum in cooling in the lower stratosphere and a larger peak in the upper stratosphere (see Figure 1 of Shine et al., 2003). The latter effect is particularly evident in the modeled temperature trends over the period 1979–1997 (Figure 3b) when ozone depletion was increasing with time. Global stratospheric cooling has continued at levels above ~60 hPa since 1998, approximately when atmospheric concentrations of halogenated ODSs began to decline (e.g., WMO, 2014), but the magnitude of cooling is weaker and the vertical profile shows a more gradual increase with height (Figure 3c) compared to the earlier period, consistent with the dominant effect of GHGs on stratospheric temperatures since ~1998. This can also be seen in the CCMI experiments with
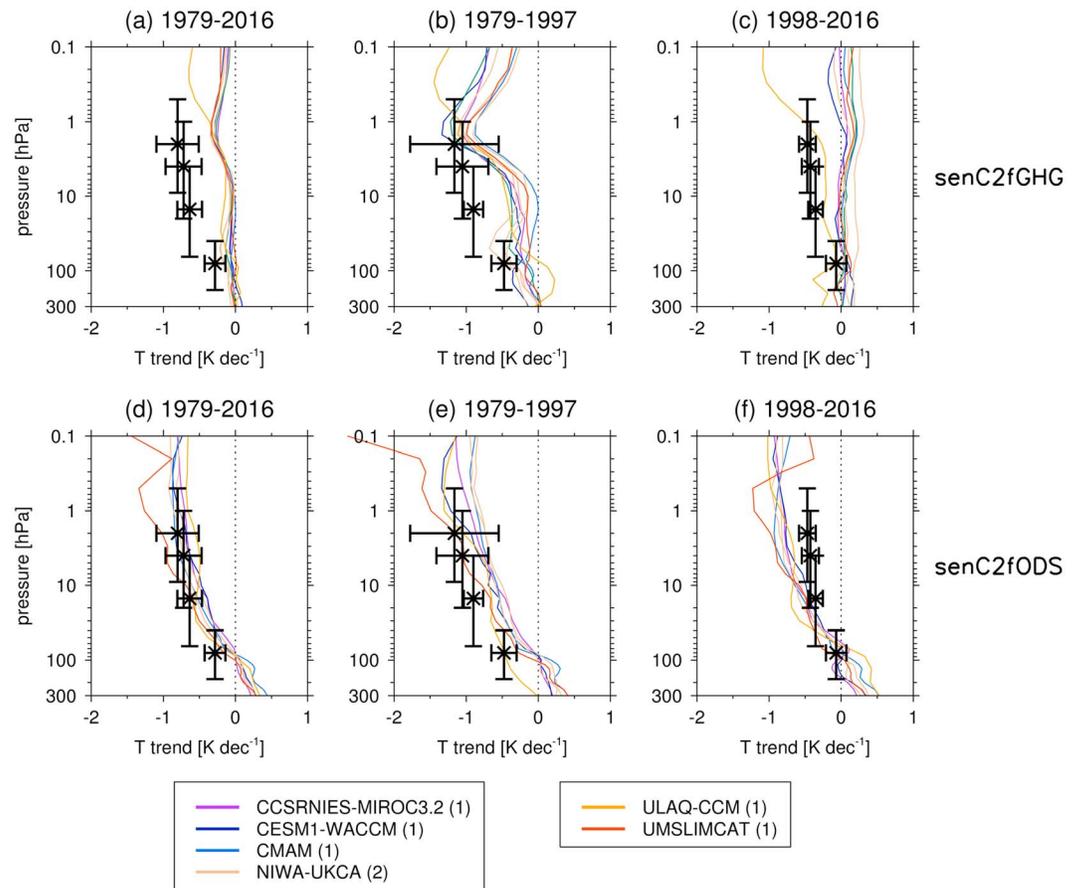
Figure 4. As in Figure 3, but for the CCMI (a–c) fixed 1960 greenhouse gases (senC2fGHG) and (d–f) fixed 1960 ODSs (senC2fODS) experiments. CCMI = Chemistry-Climate Model Initiative.

GHG concentrations fixed at 1960 levels (senC2fGHG) and with ODS concentrations fixed at 1960 levels (senC2fODS; Figure 4). When GHG concentrations are fixed at 1960 levels, the models show substantially weaker temperature trends in the middle and upper stratosphere over 1998–2016 with a small warming in the upper stratosphere (Figure 4c), which is presumably related to increases in upper stratospheric ozone over this period (Harris et al., 2015). In contrast, when increases in GHGs are considered but ODSs are fixed at 1960 levels (Figure 4f), the models capture the observed cooling in the middle and upper stratosphere over 1998–2016. ULAQ-CCM is the exception as it appears to show stronger stratospheric cooling over 1998–2016 when GHGs are fixed at 1960 levels (Figure 4c); this is likely the result of the model simulating strong quasi-decadal variability in stratospheric temperatures likely related to the solar cycle, (see section 3.1) and because the start and end points of the trend period are close to a maximum and minimum phase of the 11-year solar cycle, respectively. Near 1 hPa, the CCMI models show approximately equal contributions to cooling over 1979–1997 from ODSs (Figure 4b) and GHGs (Figure 4e), consistent with earlier attribution studies (e.g., Shine et al., 2003). In the middle stratosphere (7–30 hPa), cooling over 1979–1997 was dominated by the effects of GHGs (see also Shine et al., 2003, Figures 1 and 2). In summary, the CCMI models simulate significantly smaller stratospheric temperature trends over 1998–2016 compared to 1979–1997, which are consistent with estimates from satellite data sets (see also Randel et al., 2016, 2017; Zou and Qian, 2016).

3.2. Spatial and Seasonal Characteristics of Stratospheric Temperature Trends

The differences in stratospheric temperature trends between model simulations and satellite data sets discussed by Thompson et al. (2012) were largest across the tropics and subtropics. Subsequent analysis has found greater consistency in the spatial pattern of stratospheric temperature trends between the updated NOAA/STAR SSU data set and the CESM1(WACCM) model (Randel et al., 2017), though analysis of multiple
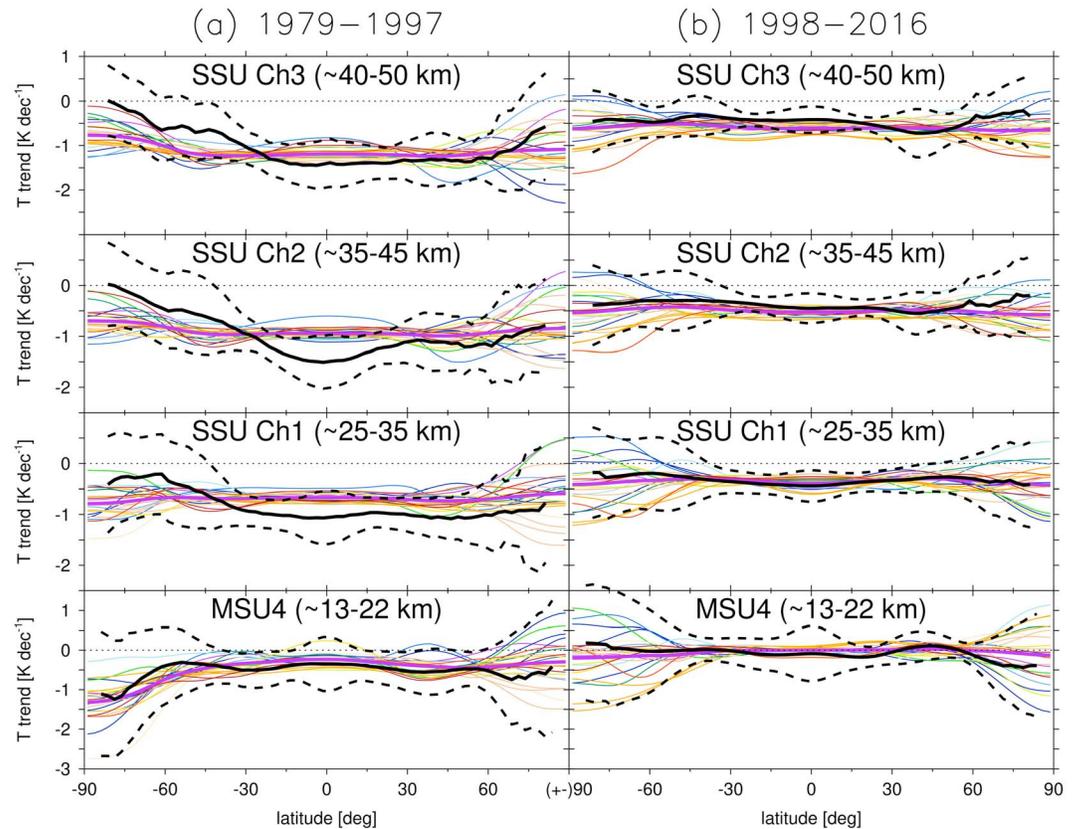
Figure 5. Latitudinal profiles of annual temperature trends (K/decade) over the 19-year periods (a) 1979–1997 and (b) 1998–2016 in the NOAA/STAR satellite data set (black) and CCMI simulations. Colors and the number of individual ensemble members plotted for each model are as in Figure 1. The dashed black lines denote the 95% confidence intervals on the observed trends. Note the different *y* axis ranges in the subpanels. NOAA/STAR = National Oceanographic and Atmospheric Administration Center for Satellite Applications and Research; CCMI = Chemistry-Climate Model Initiative.

ensemble members reveals that larger differences in trends can occur at high latitudes due to the effects of internal atmospheric variability. Figure 5 shows trends in monthly mean SSU and MSU4 layer temperatures as a function of latitude for the periods 1979–1997 (Figure 5a) and 1998–2016 (Figure 5b) in the CCMI models and satellite data sets. Note that for the MSU4 channel the three satellite records shown in Figure 1 exhibit similar patterns of trends (not shown; see also Seidel et al., 2016).

The range of CCMI modeled trends overlap the 95% confidence intervals of the satellite observed trends at all latitudes and in both time periods. Note that one should not expect the multimodel mean to match the observed trends exactly, because the former implicitly smooths the effects of internal atmospheric variability, while the observations essentially reflect a single realization of the atmosphere. Note therefore that the confidence intervals on the observations only account for uncertainties due to interannual variability which affect the regression fit and do not capture any contribution to uncertainty from internal atmospheric variability, while the intermodel spread reflects both structural differences between models and the effects of internal atmospheric variability.

The models with multiple ensemble members enable an assessment of the potential contribution of internal atmospheric variability to observed stratospheric temperature trends. In the tropics, the differences in trends between ensemble members from the same model are less than ~0.1–0.2 K/decade. However, in the polar regions the differences in trends between ensemble members can be as large as 0.5 K/decade. Large inter-ensemble spread in stratospheric temperature trends at high latitudes was found by Randel et al. (2017) for the CESM1(WACCM) model, and similar results are found here for additional CCMI models.

The analysis so far has focused on stratospheric temperature trends across all months. However, stratospheric ozone trends, as a major contributor to past stratospheric temperature trends, show strong spatial and
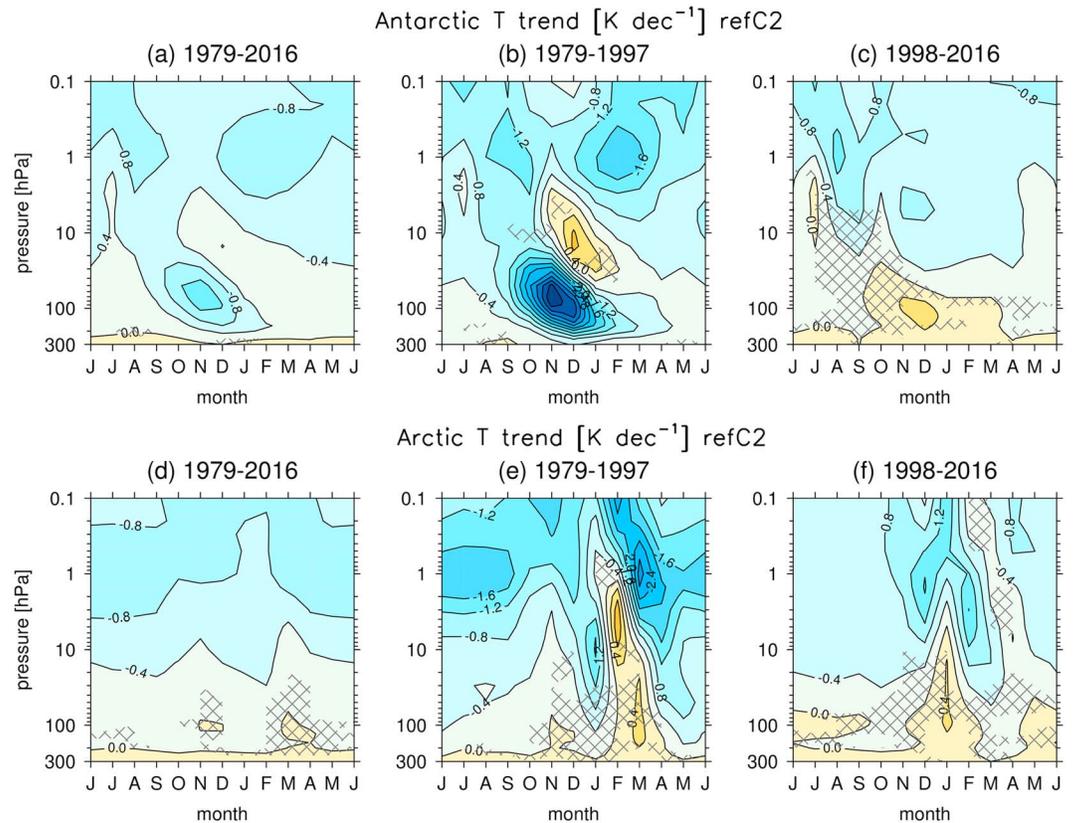
Figure 6. CCMI multimodel mean polar temperature trends (K/decade) as a function of month for the periods (a, d) 1979–2016, (b, e) 1979–1997, and (c, f) 1998–2016. (a–c) Shows the Antarctic (70–90°S) and (d–f) shows the Arctic (70–90°N). The contour interval is 0.4 K/decade. The hatching shows where fewer than 10 out 14 models agree on the sign of the trend. CCMI = Chemistry-Climate Model Initiative.

seasonal structure (e.g., WMO, 2014). A strong seasonality in polar stratospheric temperature trends has also been shown in reanalysis data sets (Bohlinger et al., 2014; Garfinkel et al., 2015; Ivy et al., 2016; Thompson & Solomon, 2002) and model simulations (e.g., Calvo et al., 2017; Keeble et al., 2014; Orr et al., 2013). Figure 6 shows CCMI multimodel mean polar cap (70–90°) average temperature trends as a function of pressure and month for the Antarctic (Figures 6a–6c) and the Arctic (Figures 6d–6f) for three time periods: 1979–2016, 1979–1997, and 1998–2016. The hatching denotes regions where fewer than 10 models out of 14 (~65%) agree on the sign of the trend. Over the period 1979–2016, the CCMI multimodel mean shows stratospheric cooling throughout most of the year that increases in magnitude with height in both the Antarctic and Arctic (Figures 6a and 6d). Superposed on this in the Antarctic is a seasonal signature of enhanced lower stratospheric cooling in austral spring and summer (e.g., Thompson & Solomon, 2002), with warming in the middle stratosphere in summer that has been shown to be of dynamical origin (e.g., Orr et al., 2013; Rosier & Shine, 2000). This pattern is strongly enhanced for the period 1979–1997 when the largest trends in Antarctic ozone depletion occurred, and since 1998 the trends are substantially smaller and even show a small warming in the Antarctic lower stratosphere in spring/early summer, which may be associated with the onset of recovery of the ozone hole, as has been reported in the CESM1(WACCM) model (Randel et al., 2017; Solomon et al., 2017). In the Arctic, temperature trends over the period 1979–2016 do not show a strong seasonality (Figure 6d). Over 1979–1997, the trends suggest a warming of the Arctic upper stratosphere (~1–20 hPa) in late winter and a cooling throughout the stratosphere in spring (Figure 6e). However, there is a large spread in Arctic lower stratospheric temperature trends in winter across the models (see Figure S2 in the supporting information), with the multimodel mean reflecting only a small residual (~|0.5| K/decade in MSU4 layer) from the averaging of large (~|2–5|K/decade in MSU4 layer) and opposing trends in the different models. This is perhaps unsurprising given the large internal variability in the Arctic winter stratosphere (e.g., Maycock &

Hitchcock, 2015) and the relatively short period of the trends (19 years, Figures 6e and 6f). Reanalysis data sets show a midwinter warming and a late winter cooling in the Arctic stratosphere over the period 1980–2000 (Ivy et al., 2016). Given the large spread in Arctic winter temperature trends across the models, it seems plausible that the reanalysis *trends* are likely to at least partly reflect internal atmospheric variability, though part of the early springtime lower stratospheric cooling over 1980–2009 may be related to SST trends (which could themselves have both a forced and unforced component; Garfinkel et al., 2015).

4. Conclusions

Thompson et al. (2012) highlighted substantial discrepancies in stratospheric temperature trends between previous versions of the SSU satellite record developed by the Met Office and NOAA/STAR, as well as between model-simulated and satellite-derived stratospheric temperature trends. This study provides an update to these previous findings in light of the recently reprocessed versions of the SSU temperature records (Nash & Saunders, 2015; Seidel et al., 2016; Zou & Qian, 2016) and new model simulations performed by the IGAC/SPARC Chemistry Climate Model Initiative (CCMI; Eyring et al., 2013). The results show substantial improvements in the agreement between modeled and observed stratospheric temperature trends in the altitude ranges sampled by the SSU channels. This improvement comes largely from changes to the satellite derived trends rather than from significant changes to the modeled trends, which remain similar to earlier generations of models. The estimated CCMI multimodel mean temperature trends over 1979–2005 with 95% confidence intervals are -0.25 ± 0.12 (MSU4, ~13–22 km), -0.50 ± 0.12 (SSU channel 1, ~25–35 km), -0.70 ± 0.16 (SSU channel 2, ~35–45 km), and -0.88 ± 0.23 (SSU channel 3, ~40–50 km) K/decade. These are within the estimated uncertainty ranges of the trends derived from the most recent versions of the satellite data sets. The models simulate weaker global stratospheric cooling in the SSU channels over 1998–2016 compared to 1979–1997 and nonsignificant temperature trends in the lower stratosphere (MSU4) over the latter period, comparable to observations (Ferraro et al., 2015; Khaykin et al., 2017). However, in the tropics one should keep in mind that the MSU4 integrates over the lower stratosphere and upper troposphere and hence includes some effects of tropospheric warming (Ladstädter et al., 2011; Randel et al., 2009). In this region, vertically resolved observations from GPS radio occultation are well suited for trend analysis in the postmillennium period (e.g., Ladstädter et al., 2015; Steiner et al., 2011, 2013), and future studies could make further use of this record as it becomes long enough to distinguish long-term trends. The latitudinal structure of temperature trends between the models and observations are also consistent within their estimated uncertainties over the periods 1979–1997 and 1998–2016. CCMI experiments designed to separate the effects of changes in atmospheric ODSs and other long-lived greenhouse gases indicate that GHGs made a dominant contribution to global stratospheric temperature trends over 1998–2016, while both ODSs (via their effect on ozone) and GHGs made comparable contributions to cooling near 1 hPa over 1979–1997 and ODSs dominated the lower stratospheric cooling trend prior to 1997.

In summary, chemistry-climate models forced with observed changes in GHGs and ODSs, and which include other drivers of stratospheric temperature variability (e.g., solar variability), simulate long-term stratospheric temperature trends since 1979 that are in good quantitative agreement with updated and extended satellite temperature records both globally and in their latitudinal structure. These findings help to further resolve some of the issues raised by Thompson et al. (2012) around understanding of recent global stratospheric temperature trends. One outstanding issue is the degree of consistency in the latitudinal structure of observed and modeled stratospheric temperature trends. Changes in the magnitude or structure of the Brewer-Dobson circulation can imprint on the latitudinal structure of stratospheric temperature trends (e.g., Young et al., 2012). While recent progress has been made in separating the relative importance of radiative and dynamical processes for polar stratospheric temperature trends (Bohlinger et al., 2014; Ivy et al., 2016), disentangling the externally forced part of stratospheric temperature trends at different latitudes from changes associated with internal variability remains a challenge. Diagnosing the contribution of dynamical processes to recent stratospheric temperature trends is further hampered by a comparative lack of direct observational constraints on changes in the magnitude and structure of the Brewer-Dobson circulation since 1979 (e.g., WMO, 2014), though model and reanalysis studies do suggest a strengthening of the circulation over recent decades (Abalos et al., 2015; Polvani et al., 2017). In future, efforts could be made to compare modeled stratospheric ozone, water vapor, and Brewer-Dobson circulation changes in combination with stratospheric temperature trends and to explicitly diagnose their separate contributions. This could provide

AGU
100
ADVANCING EARTH
AND SPACE SCIENCE

Geophysical Research Letters

10.1029/2018GL078035

quantitative insight to the model spread in the latitudinal structure of stratospheric temperature trends described in this study. Another useful tool is model ensemble experiments that allow the role of internal variability to be investigated within a single, physically consistent (model) system in a manner that is not possible for the real atmosphere. Model studies have revealed that a large spread in polar stratospheric temperature trends can arise in members with identical external forcings solely from the effects of internal variability (e.g., Randel et al., 2017). This offers insight to the degree of consistency in the pattern of stratospheric temperature trends over a few decades that can be expected between individual model realizations and the real atmosphere.

References

Abalos, M., Legras, B., Ploeger, F., & Randel, W. J. (2015). Evaluating the advective Brewer-Dobson circulation in three reanalyses for the period 1979–2012. *Journal of Geophysical Research: Atmospheres*, *120*, 7534–7554. https://doi.org/10.1002/2015JD023182

Akiyoshi, H., Nakamura, T., Miyasaka, T., Shiotani, M., & Suzuki, M. (2016). A nudged chemistry-climate model simulation of chemical constituent distribution at northern high-latitude stratosphere observed by SMILES and MLS during the 2009/2010 stratospheric sudden warming. *Journal of Geophysical Research: Atmospheres*, *121*, 1361–1380. https://doi.org/10.1002/2015JD023334

Aquila, V., Swartz, W. H., Waugh, D. W., Colarco, P. R., Pawson, S., Polvani, L. M., & Stolarski, R. S. (2016). Isolating the roles of different forcing agents in global stratospheric temperature changes using model integrations with incrementally added single forcings. *Journal of Geophysical Research: Atmospheres*, *121*, 8067–8082. https://doi.org/10.1002/2015JD023841

Arblaster, J. M., Gillett, N. P., Calvo, N., Forster, P. M., Polvani, L. M., Son, S.-W., et al. (2014). Stratospheric ozone changes and climate. In *Chapter 4 in Scientific assessment of ozone depletion: 2014, Global Ozone Research and Monitoring Project-Report No. 55* (Chap. 4, 61 pp.). Geneva, Switzerland: World Meteorological Organization.

Austin, J., Wilson, R. J., Akiyoshi, H., Bekki, S., Butchart, N., Claud, C., et al. (2009). Coupled chemistry climate model simulations of stratospheric temperatures and their trends for the recent past. *Geophysical Research Letters*, *36*, L13809. https://doi.org/10.1029/2009GL038462

Bednarz, E. M., Maycock, A. C., Abraham, N. L., Braesicke, P., Dessens, O., & Pyle, J. A. (2016). Future Arctic ozone recovery: The importance of chemistry and dynamics. *Atmospheric Chemistry and Physics*, *16*(18), 12159–12176. https://doi.org/10.5194/acp-16-12159-2016

Bohlinger, P., Sinnhuber, B.-M., Ruhnke, R., & Kirner, O. (2014). Radiative and dynamical contributions to past and future Arctic stratospheric temperature trends. *Atmospheric Chemistry and Physics*, *14*, 1679–1688. https://doi.org/10.5194/acp-14-1679-2014

Calvo, N., Garcia, R. R., & Kinnison, D. E. (2017). Revisiting Southern Hemisphere polar stratospheric temperature trends in WACCM: The role of dynamical forcing. *Geophysical Research Letters*, *44*, 3402–3410. https://doi.org/10.1002/2017GL072792

Christy, J. R., Spencer, R. W., Norris, W. B., & Braswell, W. D. (2003). Error estimates of version 5.0 of MSU-AMSU bulk atmospheric temperature. *Journal of Atmospheric and Oceanic Technology*, *20*(5), 613–629. https://doi.org/10.1175/1520-0426(2003)20%3C613:EEOVOM%3E2.0.CO;2

Forster, P. M. de F., & Shine, K. P. (1999). Stratospheric water vapour changes as a possible contributor to observed stratospheric cooling. *Geophysical Research Letters*, *26*(21), 3309–3312. https://doi.org/10.1029/1999GL010487

Deushi, M., & Shibata, K. (2011). Development of a Meteorological Research Institute chemistry-climate model version 2 for the study of tropospheric and stratospheric chemistry. *Papers in Meteorology and Geophysics*, *62*, 1–46. https://doi.org/10.2467/mripapers.62.1

Eyring, V., Lamarque, J.-F., Hess, P., Arfeuille, F., Bowman, K., Chipperfield, M. P., et al. (2013). Overview of IGAC/SPARC Chemistry-Climate Model Initiative (CCMI) community simulations in support of upcoming ozone and climate assessments, SPARC Newsletter 40.

Ferraro, A. J., Collins, M., & Lambert, F. H. (2015). A hiatus in the stratosphere. *Nature Climate Change*, *5*(6), 497–498. https://doi.org/10.1038/nclimate2624

Garfinkel, C. I., Hurwitz, M. M., & Oman, L. D. (2015). Effect of recent sea surface temperature trends on the Arctic stratospheric vortex. *Journal of Geophysical Research: Atmospheres*, *120*, 5404–5416. https://doi.org/10.1002/2015JD023284

Garfinkel, C. I., Son, S.-W., Song, K., Aquila, V., & Oman, L. D. (2017). Stratospheric variability contributed to and sustained the recent hiatus in Eurasian winter warming. *Geophysical Research Letters*, *44*, 374–382. https://doi.org/10.1002/2016GL072035

Gillett, N. P., & Thompson, D. W. J. (2003). Simulation of recent Southern Hemisphere climate change. *Science*, *302*(5643), 273–275. https://doi.org/10.1126/science.1087440

Hardiman, S. C., Butchart, N., O'Connor, F. M., & Rumbold, S. T. (2017). The Met Office HadGEM3-ES Chemistry-Climate Model: Evaluation of stratospheric dynamics and its impact on ozone. *Geoscientific Model Development*, *10*, 1–40. https://doi.org/10.5194/gmd-2016-276

Harris, N. R. P., Hassler, B., Tummon, F., Bodeker, G. E., Hubert, D., Petropavlovskikh, I., et al. (2015). Past changes in the vertical distribution of ozone—Part 3: Analysis and interpretation of trends. *Atmospheric Chemistry and Physics*, *15*, 9965–9982. https://doi.org/10.5194/acp-15-9965-2015

Hartmann, D. L., Klein Tank, A. M. G., Rusticucci, M., Alexander, L. V., Brönnimann, S., Charabi, Y., et al. (2013). Observations: atmosphere and surface. In T. F. Stocker, D. Qin, G.-K. Plattner, M. Tignor, S. K. Allen, J. Boschung, et al. (Eds.), *Climate Change 2013: The Physical Science Basis. Contribution of Working Group I to the Fifth Assessment Report of the Intergovernmental Panel on Climate Change*. Cambridge, UK and New York: Cambridge University Press.

Hunke, E. C., & Lipscombe, W. H. (2008). CICE: The Los Alamos sea ice model documentation and software user's manual, Version 4.0, LA-CC-06-012, Los Alamos National The Laboratory, New Mexico.

Imai, K., Manago, N., Mitsuda, C., Naito, Y., Nishimoto, E., Sakazaki, T., et al. (2013). Validation of ozone data from the Superconducting Submillimeter-Wave Limb-Emission Sounder (SMILES). *Journal of Geophysical Research: Atmospheres*, *118*, 5750–5769. https://doi.org/10.1002/jgrd.50434

Ivy, D. J., Solomon, S., & Rieder, H. E. (2016). Radiative and dynamical influences on polar stratospheric temperature trends. *Journal of Climate*, *29*, 4927–4938. https://doi.org/10.1175/JCLI-D-15-0503.1

Jöckel, P., Tost, H., Pozzer, A., Kunze, M., Kirner, O., Brenninkmeijer, C. A. M., et al. (2016). Earth System Chemistry integrated Modelling (ESCiMo) with the Modular Earth Submodel System (MESSy) version 2.51. *Geoscientific Model Development*, *9*, 1153–1200. https://doi.org/10.5194/gmd-9-1153-2016

Jonsson, A. I., de Grandpré, J., Fomichev, V. I., McConnell, J. C., & Beagley, S. R. (2004). Doubled CO_2-induced cooling in the middle atmosphere: Photochemical analysis of the ozone radiative feedback. *Journal of Geophysical Research*, *109*, D24103. https://doi.org/10.1029/2004JD005093

Keeble, J., Braesicke, P., Abraham, N. L., Roscoe, H. K., & Pyle, J. A. (2014). The impact of polar stratospheric ozone loss on Southern Hemisphere stratospheric circulation and climate. *Atmospheric Chemistry and Physics*, *14*, 13,705–13,717. https://doi.org/10.5194/acp-14-13705-2014

Khaykin, S. M., Funatsu, B. M., Hauchecorne, A., Godin-Beekmann, S., Claud, C., Keckhut, P., et al. (2017). Postmillennium changes in stratospheric temperature consistently resolved by GPS radio occultation and AMSU observations. *Geophysical Research Letters*, *44*, 7510–7518. https://doi.org/10.1002/2017GL074353

Ladstädter, F., Steiner, A. K., Foelsche, U., Haimberger, L., Tavolato, C., & Kirchengast, G. (2011). An assessment of differences in lower stratospheric temperature records from (A)MSU, radiosondes, and GPS radio occultation. *Atmospheric Measurement Techniques*, *4*(9), 1965–1977. https://doi.org/10.5194/amt-4-1965-2011

Ladstädter, F., Steiner, A. K., Schwärz, M., & Kirchengast, G. (2015). Climate intercomparison of GPS radio occultation, RS90/92 radiosondes and GRUAN from 2002 to 2013. *Atmospheric Measurement Techniques*, *8*(4), 1819–1834. https://doi.org/10.5194/amt-8-1819-2015

Lary, D. J., Balluch, M., & Bekki, S. (1994). Solar heating rates after a volcanic eruption: The importance of SO_2 absorption. *Quarterly Journal of the Royal Meteorological Society*, *120*(520), 1683–1688. https://doi.org/10.1002/qj. 49712052011

Madec, G. (2008). *NEMO ocean engine* (Vol. 27). France: Institut Piere-Simon Laplace (IPSL).

Manabe, S., & Wetherald, R. T. (1975). The effects of doubling the CO_2 concentration on the climate of a general circulation model. *Journal of the Atmospheric Sciences*, *32*, 3–15. https://doi.org/10.1175/1520-0469(1975)032%3C0003:TEODTC%3E2.0.CO;2

Marsh, D., Mills, M. J., Kinnison, D. E., Garcia, R. R., Lamarque, J.-F., & Calvo, N. (2013). Climate change from 1850–2005 simulated in CESM1 (WACCM). *Journal of Climate*, *26*(19), 7372–7391. https://doi.org/10.1175/JCLI-D-12-00558.1

Maycock, A. C., & Hitchcock, P. (2015). Do split and displacement sudden stratospheric warmings have different annular mode signatures? *Geophysical Research Letters*, *42*, 10,943–10,951. https://doi.org/10.1002/2015GL066754

Maycock, A. C., Joshi, M. M., Shine, K. P., Davis, S. M., & Rosenlof, K. H. (2014). The potential impact of changes in lower stratospheric water vapour on stratospheric temperatures over the past 30 years. *Quarterly Journal of the Royal Meteorological Society*, *140*(684), 2176–2185. https://doi.org/10.1002/qj.2287

McLandress, C., Shepherd, T. G., Jonsson, A. I., von Clarmann, T., & Funke, B. (2015). A method for merging nadir-sounding climate records, with an application to the global-mean stratospheric temperature data sets from SSU and AMSU. *Atmospheric Chemistry and Physics*, *15*(16), 9271–9284. https://doi.org/10.5194/acp-15-9271-2015

Mears, C. A., & Wentz, F. J. (2009). Construction of the remote sensing systems V3.2 atmospheric temperature records from the MSU and AMSU microwave sounders. *Journal of Atmospheric and Oceanic Technology*, *26*(6), 1040–1056. https://doi.org/10.1175/2008JTECHA1176.1

Mears, C. A., Wentz, F. J., Thorne, P., & Bernie, D. (2011). Assessing uncertainty in estimates of atmospheric temperature changes from MSU and AMSU using a Monte-Carlo estimation technique. *Journal of Geophysical Research*, *116*, D08112. https://doi.org/10.1029/2010JD014954

Michou, M., Saint-Martin, D., Teyssèdre, H., Alias, A., Karcher, F., Olivié, D., et al. (2011). A new version of the CNRM Chemistry-Climate Model, CNRM-CCM: Description and improvements from the CCMVal-2 simulations. *Geoscientific Model Development*, *4*(4), 873–900. https://doi.org/10.5194/gmd-4-873-2011

Mitchell, D. M. (2016). Attributing the forced components of observed stratospheric temperature variability to external drivers. *Quarterly Journal of the Royal Meteorological Society*, *142*(695), 1041–1047. https://doi.org/10.1002/qj.2707

Molod, A., Takacs, L., Suarez, M., & Bacmeister, J. (2015). Development of the GEOS-5 atmospheric general circulation model: Evolution from MERRA to MERRA2. *Geoscientific Model Development*, *8*(5), 1339–1356. https://doi.org/10.5194/gmd-8-1339-2015

Molod, A., Takacs, L., Suarez, M., Bacmeister, J., Song, I.-S., & Eichmann, A. (2012). The GEOS-5 Atmospheric General Circulation Model: Mean climate and development from MERRA to Fortuna, NASA Technical Report Series on Global Modeling and Data Assimilation, NASA TM-2012-104606 (Vol. 28, 117 pp.).

Morgenstern, O., Braesicke, P., O'Connor, F. M., Bushell, A. C., Johnson, C. E., Osprey, S. M., & Pyle, J. A. (2009). Evaluation of the new UKCA climate-composition model—Part 1: The stratosphere. *Geoscientific Model Development*, *2*(1), 43–57. https://doi.org/10.5194/gmd-2-43-2009

Morgenstern, O., Hegglin, M. I., Rozanov, E., O'Connor, F. M., Abraham, N. L., Akiyoshi, H., et al. (2017). Review of the global models used within phase 1 of the Chemistry–Climate Model Initiative (CCMI). *Geoscientific Model Development*, *10*, 639–671. https://doi.org/10.5194/gmd-10-639-2017

Morgenstern, O., Zeng, G., Abraham, N. L., Telford, P. J., Braesicke, P., Pyle, J. A., et al. (2013). Impacts of climate change, ozone recovery, and increasing methane on surface ozone and the tropospheric oxidizing capacity. *Journal of Geophysical Research: Atmospheres*, *118*, 1028–1041. https://doi.org/10.1029/2012JD018382

Nash, J., & Saunders, R. (2013). A review of stratospheric sounding unit radiance observations in support of climate trends investigations and reanalysis, Met Office Technical Report 586 (pp. 58). Retrieved from https://www.metoffice.gov.uk/binaries/content/assets/mohippo/pdf/1/r/frtr_586.pdf

Nash, J., & Saunders, R. (2015). A review of stratospheric sounding unit radiance observations for climate trends and reanalyses. *Quarterly Journal of the Royal Meteorological Society*, *141*(691), 2103–2113. https://doi.org/10.1002/qj.2505

O'Connor, F. M., Johnson, C. E., Morgenstern, O., Abraham, N. L., Braesicke, P., Dalvi, M., et al. (2014). Evaluation of the new UKCA climate-composition model—Part 2: The troposphere. *Geoscientific Model Development*, *7*(1), 41–91. https://doi.org/10.5194/gmd-7-41-2014

Oman, L. D., Douglass, A. R., Ziemke, J. R., Rodriguez, J. M., Waugh, D. W., & Nielsen, J. E. (2013). The ozone response to ENSO in Aura satellite measurements and a chemistry-climate simulation. *Journal of Geophysical Research: Atmospheres*, *118*, 965–976. https://doi.org/10.1029/2012JD018546

Oman, L. D., Ziemke, J. R., Douglass, A. R., Waugh, D. W., Lang, C., Rodriguez, J. M., & Nielsen, J. E. (2011). The response of tropical tropospheric ozone to ENSO. *Geophysical Research Letters*, *38*, L13706. https://doi.org/10.1029/2011GL047865

Orr, A., Bracegirdle, T. J., Hosking, J. S., Feng, W., Roscoe, H. K., & Haigh, J. D. (2013). Strong dynamical modulation of the cooling of the polar stratosphere associated with the Antarctic ozone hole. *Journal of Climate*, *26*(2), 662–668. https://doi.org/10.1175/JCLI-D-12-00480.1

Pitari, G., Aquila, V., Kravitz, B., Robock, A., Watanabe, S., Cionni, I., et al. (2014). Stratospheric ozone response to sulfate geoengineering: Results from the Geoengineering Model Intercomparison Project (GeoMIP). *Journal of Geophysical Research: Atmospheres*, *119*, 2629–2653. https://doi.org/10.1002/2013JD020566

Polvani, L. M., Wang, L., Aquila, V., & Waugh, D. W. (2017). The impact of ozone-depleting substances on tropical upwelling, as revealed by the absence of lower-stratospheric cooling since the late 1990s. *Journal of Climate*, *30*(7), 2523–2534. https://doi.org/10.1175/JCLI-D-16-0532.1

Randel, W. J., Polvani, L., Wu, F., Kinnison, D. E., Zou, C.-Z., & Mears, C. (2017). Troposphere-stratosphere temperature trends derived from satellite data compared with ensemble simulations from WACCM. *Journal of Geophysical Research: Atmospheres*, *122*, 9651–9667. https://doi.org/10.1002/2017JD027158

Randel, W. J., Shine, K. P., Austin, J., Barnett, J., Claud, C., Gillett, N. P., et al. (2009). An update of observed stratospheric temperature trends. *Journal of Geophysical Research*, *114*, D02107. https://doi.org/10.1029/2008JD010421

Randel, W. J., Smith, A. K., Wu, F., Zou, C.-Z., & Qian, H. (2016). Stratospheric temperature trends over 1979–2015 derived from combined SSU, MLS and SABER satellite observations. *Journal of Climate*, *29*(13), 4843–4859. https://doi.org/10.1175/JCLI-D-15-0629.1

Revell, L. E., Tummon, F., Stenke, A., Sukhodolov, T., Coulon, A., Rozanov, E., et al. (2015). Drivers of the tropospheric ozone budget throughout the 21st century under the medium-high climate scenario RCP 6.0. *Atmospheric Chemistry and Physics*, *15*(10), 5887–5902. https://doi.org/10.5194/acp-15-5887-2015

Rosier, S. M., & Shine, K. P. (2000). The effect of two decades of ozone change on stratospheric temperature as indicated by a general circulation model. *Geophysical Research Letters*, *27*(17), 2617–2620. https://doi.org/10.1029/2000GL011584

Santer, B. D., Painter, J. F., Bonfils, C., Mears, C. A., Solomon, S., Wigley, T. M. L., et al. (2013). Human and natural influences on the changing thermal structure of the atmosphere. *Proceedings of the National Academy of Sciences*, *110*(43), 17,235–17,240. https://doi.org/10.1073/pnas.1305332110

Santer, B. D., Wigley, T. M. L., Boyle, J. S., Gaffen, D. J., Hnilo, J. J., Nychka, D., et al. (2000). Statistical significance of trends and trend differences in layer-average temperature time series. *Journal of Geophysical Research*, *105*(D6), 7337–7356. https://doi.org/10.1029/1999JD901105

Scinocca, J. F., McFarlane, N. A., Lazare, M., Li, J., & Plummer, D. (2008). Technical note: The CCCma third generation AGCM and its extension into the middle atmosphere. *Atmospheric Chemistry and Physics*, *8*(23), 7055–7074. https://doi.org/10.5194/acp-8-7055-2008

Seidel, D. J., Li, J., Mears, C., Moradi, I., Nash, J., Randel, W. J., et al. (2016). Stratospheric temperature changes during the satellite era. *Journal of Geophysical Research: Atmospheres*, *121*, 664–681. https://doi.org/10.1002/2015JD024039

Shine, K. P., Bourqui, M. S., Forster, P. M. d. F., Hare, S. H. E., Langematz, U., Braesicke, P., et al. (2003). A comparison of model-simulated trends in stratospheric temperatures. *Quarterly Journal of the Royal Meteorological Society*, *129*(590), 1565–1588. https://doi.org/10.1256/qj.02.186

Solomon, S., Ivy, D., Gupta, M., Bandoro, J., Santer, B., Fu, Q., et al. (2017). Mirrored changes in Antarctic ozone and stratospheric temperature in the late 20th versus early 21st centuries. *Journal of Geophysical Research: Atmospheres*, *122*, 8940–8950. https://doi.org/10.1002/2017JD026719

Solomon, S., Kinnison, D. E., Bandoro, J., & Garcia, R. (2015). Simulations of polar ozone depletion: An update. *Journal of Geophysical Research*, *120*, 7958–7974. https://doi.org/10.1002/2015JD023365

Steiner, A. K., Hunt, D., Ho, S.-P., Kirchengast, G., Mannucci, A. J., Scherllin-Pirscher, B., et al. (2013). Quantification of structural uncertainty in climate data records from GPS radio occultation. *Atmospheric Chemistry and Physics*, *13*(3), 1469–1484. https://doi.org/10.5194/acp-13-1469-2013

Steiner, A. K., Lackner, B. C., Ladstädter, F., Scherllin-Pirscher, B., Foelsche, U., & Kirchengast, G. (2011). GPS radio occultation for climate applications. *Radio Science*, *46*, RS0D24. https://doi.org/10.1029/2010RS004614

Stenke, A., Schraner, M., Rozanov, E., Egorova, T., Luo, B., & Peter, T. (2013). The SOCOL version 3.0 chemistry-climate model: Description, evaluation, and implications from an advanced transport algorithm. *Geoscientific Model Development*, *6*(5), 1407–1427. https://doi.org/10.5194/gmd-6-1407-2013

Stone, K. A., Morgenstern, O., Karoly, D. J., Klekociuk, A. R., French, W. J., Abraham, N. L., & Schofield, R. (2016). Evaluation of the ACCESS—Chemistry-climate model for the Southern Hemisphere. *Atmospheric Chemistry and Physics*, *16*, 2401–2415. https://doi.org/10.5194/acp-16-2401-2016

Thompson, D. W. J., Seidel, D. J., Randel, W. J., Zou, C.-Z., Butler, A. H., Lin, R., et al. (2012). The mystery of recent stratospheric temperature trends. *Nature*, *491*(7426), 692–697. https://doi.org/10.1038/nature11579

Thompson, D. W. J., & Solomon, S. (2002). Interpretation of recent Southern Hemisphere climate change. *Science*, *296*(5569), 895–899. https://doi.org/10.1126/science.1069270

Tian, W., & Chipperfield, M. P. (2005). A new coupled chemistry-climate model for the stratosphere: The importance of coupling for future O_3-Climate predictions. *Quarterly Journal of the Royal Meteorological Society*, *131*(605), 281–303. https://doi.org/10.1256/qj.04.05

Voldoire, A., Sanchez-Gomez, E., Salas y Mélia, D., Decharme, B., Cassou, C., Sénési, S., et al. (2013). The CNRM-CM5.1 global climate model: Description and basic evaluation. *Climate Dynamics*, *40*(9-10), 2091–2121. https://doi.org/10.1007/s00382-011-1259-y

Walters, D. N., Williams, K. D., Boutle, I. A., Bushell, A. C., Edwards, J. M., Field, P. R., et al. (2014). The Met Office Unified Model Global Atmosphere 4.0 and JULES Global Land 4.0 configurations. *Geoscientific Model Development*, *7*(1), 361–386. https://doi.org/10.5194/gmd-7-361-2014

Wang, L., Zou, C.-Z., & Qian, H. (2012). Construction of stratospheric temperature data records from stratospheric sounding units. *Journal of Climate*, *25*(8), 2931–2946. https://doi.org/10.1175/JCLI-D-11-00350.1

WMO (World Meteorological Organization) (2011). Scientific assessment of ozone depletion: 2010, Global Ozone Research and Monitoring Project–Report No. 52 (516 pp.). Geneva, Switzerland.

WMO (World Meteorological Organization) (2014). Scientific Assessment of Ozone Depletion. World Meteorological Organization, Global Ozone Research and Monitoring Project-Report No. 55 (416 pp.). Geneva, Switzerland.

Young, P. J., Rosenlof, K. H., Solomon, S., Sherwood, S. C., Fu, Q., & Lamarque, J. (2012). Changes in stratospheric temperatures and their implications for changes in the Brewer–Dobson circulation, 1979–2005. *Journal of Climate*, *25*(5), 1759–1772. https://doi.org/10.1175/2011JCLI4048.1

Yukimoto, S., Adachi, Y., Hosaka, M., Sakami, T., Yoshimura, H., Hirabara, M., et al. (2012). A new global climate model of the Meteorological Research Institute: MRI-CGCM3—Model description and basic performance. *Journal of the Meteorological Society of Japan*, *90*, 23–64.

Yukimoto, S., Yoshimura, H., Hosaka, M., Sakami, T., Tsujino, H., Hirabara, M., et al. (2011). Meteorological Research Institute Earth System Model Version 1 (MRI-ESM 1)—Model description, Tech. Rep. of MRI, 64 (83 pp.).

Zou, C.-Z., Goldberg, M., Cheng, Z., Grody, N., Sullivan, J., Cao, C., & Tarpley, D. (2006). Recalibration of microwave sounding unit for climate studies using simultaneous nadir overpasses. *Journal of Geophysical Research*, *111*, D19114. https://doi.org/10.1029/2005JD006798

Zou, C.-Z., & Qian, H. (2016). Stratospheric temperature climate data record from merged SSU and AMSU-A observations. *Journal of Atmospheric and Oceanic Technology*, *33*(9), 1967–1984. https://doi.org/10.1175/JTECH-D-16-0018.1

Zou, C.-Z., Qian, H., Wang, W., Wang, L., & Long, C. (2014). Recalibration and merging of SSU observations for stratospheric temperature trend studies. *Journal of Geophysical Research: Atmospheres*, *119*, 13,180–13,205. https://doi.org/10.1002/2014JD021603